Catalytic Oxidation of Sulfur Dioxide on Polyacrylonitrile-Based Active Hollow Carbon Fiber

MING-CHIEN YANG* and DA-GUANG YU

Department of Textile Engineering, National Taiwan Institute of Technology, Taipei, Taiwan 106, Republic of China

SYNOPSIS

The catalytic oxidation of SO_2 on polyacrylonitrile-based active hollow carbon fiber (AHCF) was investigated. A single-pass reacting system was developed to study this reaction. The sulfur dioxide contained in the gas stream was oxidized to sulfuric acid in the presence of oxygen and water. Four types of active hollow carbon fibers were prepared through various conditions in order to study the influence of the structure of AHCF on the characteristics of the catalytic oxidation. The fiber sample with more mesopores and micropores showed a higher degree of reaction, but the degree of reaction declined after a period of time, possibly due to the saturation of the active sites by the reaction products. The degree of reaction from the fiber sample with fewer mesopores and micropores did not show the overshoot and reached a steady state after a period of time. © 1996 John Wiley & Sons, Inc.

INTRODUCTION

Among the known carbon materials, the role of active carbon cannot be overlooked, either in modern industrial practice or in everyday life. Active carbon is a processed carbon material with a highly developed porous structure and a large internal specific surface area. It consists, of course, principally of carbon, but also contains such elements as hydrogen, oxygen, sulfur, and nitrogen, as well as various compounds either originating from the raw material or generated during its manufacturing.[1] Active carbons are unique and versatile adsorbents because of their extended surface area, microporous structure, high adsorption capacity, and high degree of surface reactivity.[2] They are widely used in the removal of color, odor, taste, and other undesirable organic impurities from potable water, in the treatment of domestic and industrial waste water, solvent recovery, and air pollution control in a variety of gas-phase applications. One of the major industrial applications of active carbon in the adsorption of gases is the removal from exhaust gases of toxic components containing sulfur such as sulfur dioxide, hydrogen sulfide, carbon disulfide, and organosulfur compounds.[2] Active carbon has been recognized as an excellent adsorbent for SO_2 and industrial application has been successful,[3] and for this reason, active carbon has been proposed for use in the flue gas desulfurization processes.[4] The adsorption capacity is different for each type of active carbon because it is related to the general characteristics, and, in particular, to the chemical and physical properties of the surface.[4]

The active carbons in fiber form developed recently is increasingly applied in various areas. Active carbon fibers (ACFs) have unique characteristics compared to granular or power active carbons.[5] The fibrous form is also favored because of ease in handling when it is used in membranes or hollow forms by newly developed molding techniques.

Membrane gas separation systems use asymmetric membranes in the form of hollow fiber, because high permeation flux and rate as well as high permselectivity can be achieved at the same time. Many works on the adsorption properties, morphology, and preparation techniques for polymeric hollow fibers have been reported in the literature.[6-8] In addition, efforts for the development of hollow carbon fiber (HCF) can be found in the literature.[9-13] Koresh and Soffer made HCF through pyrolysis and studied the application in gas separation.[9,10] Schindler and Maier reported a method to preserve the porous structure of the precursing PAN hollow fiber and

* To whom correspondence should be addressed.

Journal of Applied Polymer Science, Vol. 62, 2287–2293 (1996)
© 1996 John Wiley & Sons, Inc. CCC 0021-8995/96/132287-07

Table I The Effect of the Preparation Conditions on the Hydraulic Permeability of Active Hollow Carbon Fiber

Sample	Wall Structure	Dope Concentration	Activation Time (min)	Hydraulic Permeability (cm min^{-1} atm^{-1})
A	Double layer	15%	40	1.62×10^{-4}
B	Single layer	20%	40	1.43×10^{-4}
C	Double layer	15%	20	0.85×10^{-4}
D	Double layer	15%	10	0.10×10^{-4}

Oxidized at 230°C in air for 7 h, carbonized in nitrogen at 1000°C for 40 min, and activated in carbon dioxide at 800°C.

demonstrated the application of the HCF in various separation processes. Yoneyama and Nishihara showed the porous substructure of their resulting HCF with micropores ranging from 10 to 1000 nm.[12] Linkov et al. examined the surface structure of HCF with scanning probe microscopy (SPM).[13]

We recently reported the development of hollow active carbon fiber (AHCF) with PAN as the precursor material.[14-16] A previous study presented the influence of manufacturing conditions on the structure of AHCF, especially the pore-size distribution, surface area, and mechanical properties. The resulting AHCF has a thin skin layer and a porous substrate. This porous substrate can eliminate substantial resistance to gas transportation and provide AHCF with reasonable mechanical properties such as compression strength. However, the mechanical strength is necessary for the self-supporting of AHCF.

Active carbon is a catalyst for the oxidation of SO_2 in the presence of water vapor.[17] There are efforts to utilize this phenomenon to remove SO_2 from flue gas. In a series of studies, SO_2 was removed from flue gas using a trickle-bed reactor.[18-21] The reactor uses particulate active carbon as the packings. Conventionally, a larger interfacial area is created by the packings in a packed tower. However, this interface area is greatly affected by the bulk flow rates, which restricts the operation to a range of the flow rates. The flow rates of both water and gas streams in a conventional trickle bed is usually slow and is subjected to the problems of channeling, incomplete loading, or flooding. Mochida et al. reported a marked increase of SO_2 adsorption capacity on the pore walls of PAN–ACF and a pitch-based activated carbon fiber exhibited less activity than did PAN–ACF.[3,22] To overcome the flow rate re-

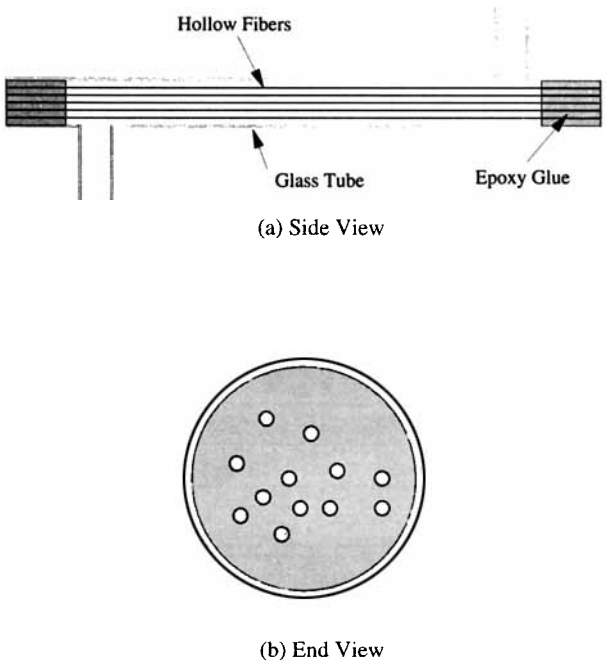

Figure 1 Schematic diagram of the structure of the hollow fiber module for measuring hydraulic permeability: (a) side view; (b) end view.

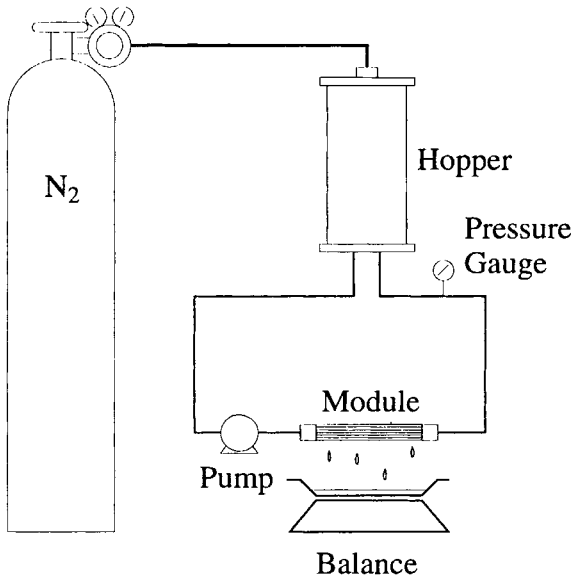

Figure 2 Schematic diagram of the experimental setup for measuring hydraulic permeability.

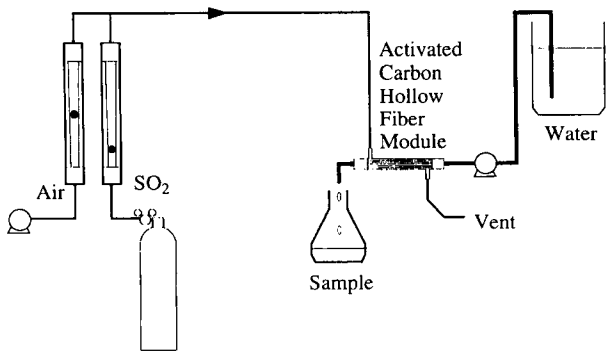

Figure 3 Schematic diagram of the experimental setup for catalytic oxidation of SO_2.

striction of the trickle-bed reactor, Yang and Cussler[23] developed a hollow-fiber trickle-bed reactor with faster reaction rates than those of the conventional trickle-bed reactor. Such a reactor has a particulate active carbon packed bed with embedded hollow fibers.

This article is a continuation to our previous works, which were aimed to preserve the membranes structure that is critical to the separation performance and practical use in gas-separation applications. In this paper, we focus on the catalytic oxidation of SO_2 using AHCF. The aim was to understand the influence of the pore structure of AHCF on the reaction rate. The results are useful for selecting the conditions for making suitable AHCFs with better catalytic power.

EXPERIMENTAL

Active Hollow Carbon Fibers

Polyacrylonitrile was obtained from Aldrich. The PAN power was first dissolved in dimehtylformamide to from dopes containing 15 or 20% of the polymer. The dope was then spun into hollow fiber through an orifice-in-tube nozzle. The resulting hollow fibers were heat-treated in air atmosphere at 230°C for 7 h, then carbonized in nitrogen at 1000°C. Afterward, the carbonized fiber was activated with carbon dioxide at 800°C for a time varying from 10 to 40 min. The details of the procedure were described in our previous articles.[14–16] The preparation conditions of the active hollow carbon fibers used in this study are listed in Table I along with their hydraulic permeabilities.

Characterization of Activated Carbon Hollow Fiber

The mechanical properties, surface area, pore-size distribution, and the composition of the AHCFs were measured as mentioned in our previous article.[14–16]

Preparation of Hollow Fiber Modules

To perform further experiments, AHCFs were packed into modules, as illustrated in Figure 1. Each module consisted 10 pieces of AHCFs of 5 cm in length. These fibers were sealed at both ends with epoxy glue. The shell was made of glass for the purpose of observation. There are two branches on the shell to allow gas or water to flow.

Determination of Hydraulic Permeability

The experimental setup for measuring hydraulic permeability (pure water permeability) of AHCFs is illustrated in Figure 2. Water in the hopper was recirculated through the lumen of the hollow fiber at a flow rate of 25 mL/min. Under a pressure of 5 psig, water was permeated through the wall of the hollow fiber. The permeate was collected and weighed to calculate the hydraulic permeability according to the following equation[24]:

$$J = AL_p\Delta P \tag{1}$$

where J is the volumetric flow rate of water (in mL/min); A, the inner surface area of the hollow fibers (in cm^2); L_p, the hydraulic permeability in ($cm\ s^{-1}\ atm^{-1}$); and ΔP, the applied pressure (in atm).

Catalytic Oxidation of SO_2 in AHCF

Figure 3 shows the experimental setup for the catalytic oxidation of SO_2 in AHCF. Water was pumped from the reservoir through the lumen of hollow fiber and collected in a flask. In the shell side of the hollow fiber module, a gas mixture of air and SO_2 flowed through. The flow rates of air and SO_2 were 45 and 5 mL/min, respectively. When SO_2 diffused through the active hollow carbon fiber, some of the molecules were oxidized into sulfuric acid, as described by the following formulas:

$$SO_{2(g)} + O_{2(g)} \xrightarrow{\text{AHCF}} SO_{3(g)} \tag{2}$$

$$SO_{3(g)} + H_2O \longrightarrow H_2SO_{4(aq)} \tag{3}$$

The reaction rate of such a single-pass reactor can be calculated from the concentration of sulfuric acid as follows[25]:

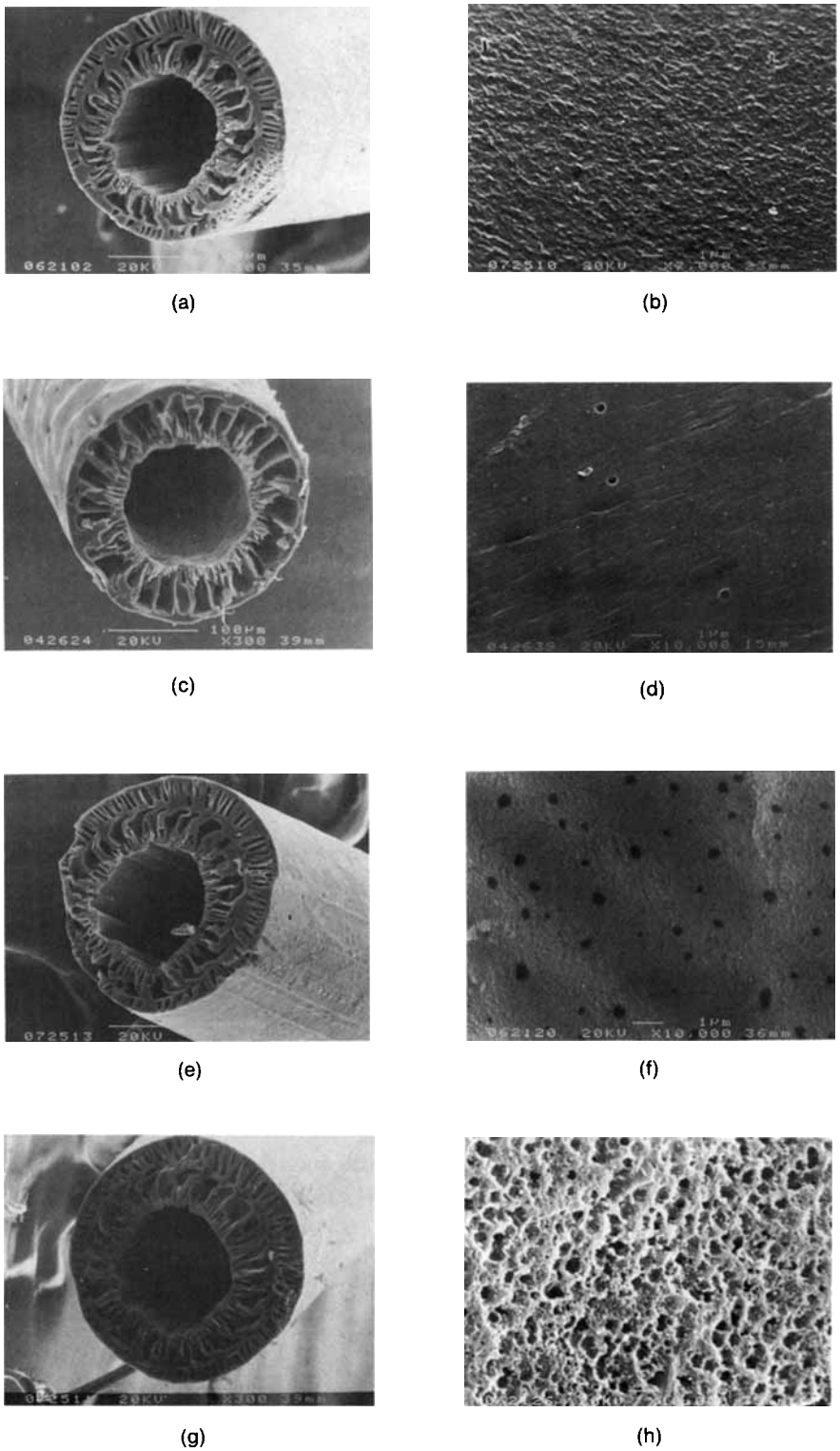

Figure 4 SEM photos of AHCF samples: (a) cross-section structure of sample A; (b) outer surface structure of sample A; (c) cross-section structure of sample B; (d) outer surface structure of sample B; (e) cross-section structure of sample C; (f) outer surface structure of sample C; (g) cross-section structure of sample D; (h) outer surface structure of sample D.

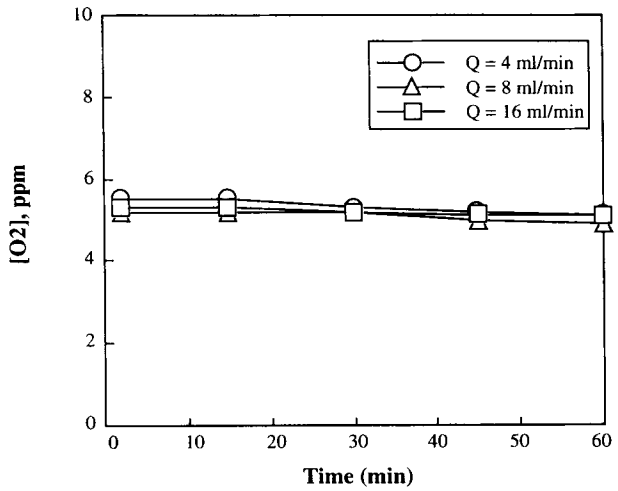

Figure 5 The variation of the concentration of dissolved oxygen in water with respect to time.

$$r = \frac{Q}{n\pi dL}[H_2SO_4] \quad (4)$$

where r is the reaction rate per unit area; Q, the flow rate of water; n, the number of fibers in the module; d, the inner diameter of AHCF; and L, the length of AHCF.

Concentration Determination of Reactants and Products

The concentration of oxygen was determined using an oxygen electrode (HI 9142, Hanna Instruments). The concentrations of those two sulfur compounds were determined by titration. The concentration of SO_2 in water was determined by the iodometric method[26] according to the following reaction:

$$SO_3^{2-} + I_2 + H_2O \rightarrow 2I^- + 2H^+ + SO_4^{2-} \quad (5)$$

The aqueous sample was mixed with hydrogen peroxide to oxidize unreacted SO_2 and was titrated with sodium hydroxide to obtain the total concentration of sulfur in water. The oxidation reaction is as follows:

$$H_2SO_3 + H_2O_2 \rightarrow H_2O + H_2SO_4 \quad (6)$$

The concentration of sulfuric acid was obtained by subtracting the concentration of SO_2 from the total concentration of sulfur. To ensure the agreement of these concentrations, the samples for either titration were from the same batch and the titrations were performed once the required liquid volume was collected.

RESULTS AND DISCUSSION

There are many factors that affect the adsorption capacity of active carbon. Two of the major factors are the chemical composition and the porosity structure of the active carbon. By the porosity structure of active carbon, we refer to the pore size and the pore-size distribution.

Wall and Surface Structure of AHCF

In Figure 4 are SEM photos for the four types of AHCF samples. Sample A has a double-layer fingerlike structure and the outer surface is full of pores of uniform size. For sample B, because of more concentrated dope, it has a single-layer fingerlike structure and the outer surface shows only very few pores. Sample C has the same double-layer finger-like structure as that of sample A, and its outer surface shows some pores. Although sample D also has a double-layer fingerlike structure, its outer surface shows only a creased surface.

Variation of Concentration of Dissolved Oxygen

Shown in Figure 5 is the time-dependent variation of the concentration of dissolved oxygen in water. We can see from the figure that during the oxidation the variation of $[O_2]$ is very small. This value is most likely the $[O_2]$ originally in the water in the reservoir. Although the saturated $[O_2]$ at 25°C was 8.3 ppm, the value of $[O_2]$ measured from the res-

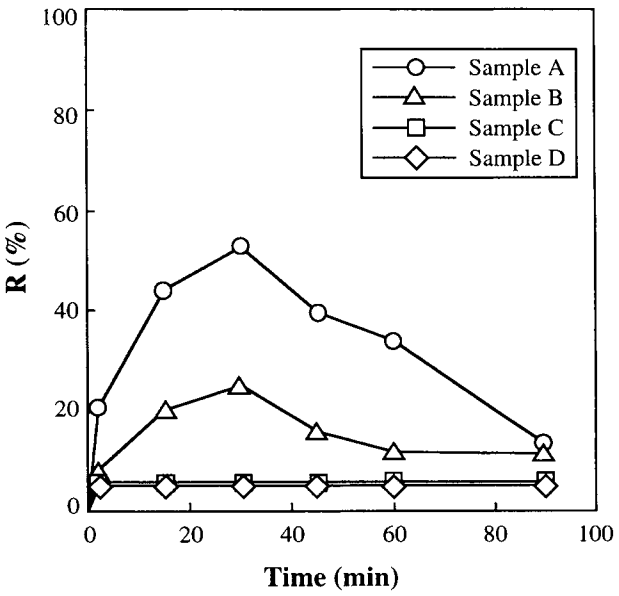

Figure 6 The variation of the degree of reaction with respect to time.

Table II The Compositions and Properties of PAN-based Active Hollow Carbon Fiber

Sample	Elemental Analysis							Surface Area (m^2/g)
	C%	H%	N%	O%	H/C%	N/C%	O/C%	
A	79.38	0.71	11.09	6.71	0.89	13.97	8.45	340
B	80.62	0.76	11.43	5.28	0.93	14.18	6.55	307
C	84.05	0.73	9.66	4.23	0.87	11.50	5.03	262
D	84.51	0.70	9.52	3.98	0.83	11.26	4.71	218

ervoir was only 5.2 ppm. In addition, the values of $[O_2]$ changed little with the liquid flow rate of the water stream. If there was any significant supply of oxygen from the gas stream, the mass-transfer rate should be proportional to the cubic root of the liquid flow rate.[22] This suggests that during the catalytic reaction the majority of O_2 came from the gas stream, since there was little consumption of dissolved oxygen.

Variation of Concentration of Sulfurous Acid

Figure 6 shows the variations of the degree of reaction of $[SO_2]$ with respect to time. The experimental data were taken at room temperature, with the gas flow rate at 5 mL/min and the liquid flow rate at 4 mL/min. We can see from the data that the degree of reaction was the greatest for sample A. This is probably because sample A has the largest specific surface area and the highest oxygen composition (see Table II). The degree of reaction reached the maximum at 30 min, then it began to decline gradually. This is probably due to the plugging of the active sites in the micropores of the active carbon by SO_2. A similar trend was observed for sample B, but with a lower degree of reaction. This is reasonable since its specific surface area is the second largest after sample A. The degree of reaction curves of samples C and D are similar, with a lower plateau reached at around 2 min.

Comparing the results of these samples, it suggests that a higher specific surface area is favored for the catalytic oxidation of SO_2. On the other hand, the rise-and-decline behavior of the degree of reaction can be attributed to the pore structure of active carbons. Samples A and B have more macropores that allow SO_2 to get into the wall; then, they diffuse to the mesopores (100–300 nm) and finally are adsorbed by those active sites in the micropores (<10 nm). With the time elapsed, SO_2 molecules cluster on the surface of micropores and occupy the active sites, thus causing the reaction to slow down. This phenomenon has been discussed by Juntgen et al.[27] When the maximum was reached, SO_2 was almost completely adsorbed by the mesopores. Ac-

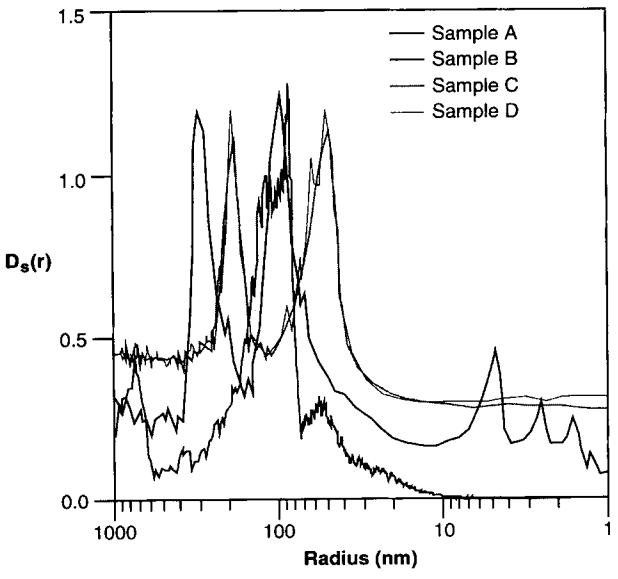

Figure 7 The pore-size distributions of AHCF samples.

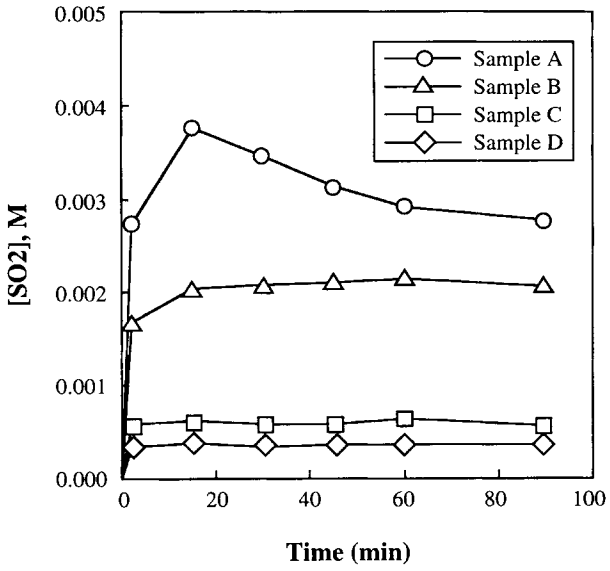

Figure 8 The variation of the concentration of sulfur dioxide in water with respect to time.

cording to Mochita et al.,[3] SO_2 is adsorbed by oxygen groups. Sample A has the highest O/C ratio and, thus, the highest degree of reaction.

Because of shorter activation time, the surface and the lumen of samples C and D suffered a lesser degree of CO_2 attacking. Their porous structure is composed of mostly macropores and mesopores. With fewer micropores and active sites, there is not enough area for SO_2 to deposit. Because sample A has more mesopores, it takes longer to saturate those pores (see Fig. 7). Yet, once the maximum is reached, the decline of the degree of reaction suggests the deposit of those micropores by SO_2. Since samples C and D have fewer micropores, there is no significant decrease in the active sites; thus, a steady-state value was observed from their experimental results.

Effect of Active Hollow Carbon Fiber on Catalytic Oxidation of SO_2

Figure 8 shows the variation of $[SO_2]$ in water with respect to time. The trends of these curves are similar to those curves in Figure 6. This suggests that the SO_2 passed through these four types of AHCF samples have similar reactions. We can see from Figures 6 and 8 that although sample A has the highest degree of reaction its activity greatly declined after 30 min. It has to be regenerated to regain the activity. Samples C and D, although having a lower degree of reaction, do not show a decline in the reactivity.

To avoid SO_2 saturation of the AHCF in a short duration, a small pore size and a narrow pore-size distribution are necessary for the fiber outer surface. The pore size of the inside and inner surface should be larger, because the water flux usually tends to be high.

CONCLUSION

Sulfur dioxide can be catalytically oxidized into sulfuric acid by an active hollow carbon fiber. The activity of the active hollow carbon fiber is influenced by the preparation conditions. The highest activity among the samples used in this study is the sample that has double-layer wall structure (from 15% dope), oxidized at 230°C for 7 h, carbonized at 1000°C in nitrogen for 40 min, and activated at 800°C in CO_2 for 40 min.

REFERENCES

1. H. Jankowska, A. Swiatkowski, and J. Choma, *Active Carbon,* Ellis Horwood, New York 1991.
2. R. C. Bansal, J. B. Donnet, and F. Stoeckli, *Active Carbon,* Marcel Dekker, New York, 1988.
3. I. Mochida, T. Hirayama, S. Kisamori, S. Kawano, and H. Fujitsu, *Langmuir,* **8,** 2290 (1992).
4. P. Davina, *Carbon,* **28,** 565 (1990).
5. M. Suzuki, *Carbon,* **32,** 577 (1994).
6. M. Henmi and T. Yoshioka, *J. Membr. Sci.,* **85,** 129 (1993).
7. T. S. Chung, E. R. Kafchinski, R. S. Kohn, P. Foley, and R. S. Straff, *J. Appl. Polym. Sci.,* **53,** 701 (1994).
8. H. Kumazawa, E. Sada, K. Nakata, N. Kawashima, S. Kataoka, and K. Tada, *J. Appl. Polym. Sci.,* **53,** 113 (1994).
9. J. E. Koresh and A. Soffer, *Separ. Sci. Technol.,* **18,** 723 (1983).
10. A. Soffer, J. E. Koresh, and S. Saggy, U.S. Pat. 4,685,940 (1987).
11. E. Schindler and F. Maier, U.S. Pat. 4,919,860 (1990).
12. H. Yoneyama and Y. Nishihara, U.S. Pat. 5,089,135 (1991).
13. V. Linkov, R. D. Sanderson, and E. P. Jacobes, *J. Mater. Sci. Lett.,* **13,** 600 (1994).
14. M.-C. Yang and D.-G. Yu, *J. Appl. Polym. Sci.,* **58,** 185 (1995).
15. M.-C. Yang and D.-G. Yu, *Text. Res. J.,* **66,** 115 (1996).
16. M.-C. Yang and D.-G. Yu, *J. Appl. Polym. Sci.,* **59,** 1725 (1996).
17. O. K. Davtyan and E. N. Ovchinikova, *Dokl. Akad. Nauk S.S.S.R.,* **104,** 857 (1955).
18. F. Berruti, R. R. Hudgins, and E. Rhodes, *Can. J. Chem. Eng.,* **62,** 644 (1984).
19. P. M. Haure, R. R. Hudgins, and P. L. Silveston, *Can. J. Chem. Eng.,* **70,** 600 (1992).
20. A. N. Stegasov, V. A. Kirillov, and P. L. Silveston, *Chem. Eng. Sci.,* **49,** 3699 (1994).
21. P. L. Silveston and R. R. Hudgins, *Can. J. Chem. Eng.,* **72,** 760 (1994).
22. S. Kisamori, K. Kuroda, S. Kawano, I. Mochida, Y. Matsumura, and M. Yoshikawa, *Energy Fuels,* **8,** 1337 (1994).
23. M.-C. Yang and E. L. Cussler, *AIChE J.,* **33,** 1754 (1987).
24. E. L. Cussler, *Diffusion,* Cambridge University Press, Cambridge, England (1985).
25. D.-G. Yu, Ph.D. thesis, Department of Textile Engineering, National Taiwan Institute of Technology, 1996.
26. D. A. Skoog, D. M. West, and F. J. Holler, *Fundamentals of Analytical Chemistry,* 6th ed., Saunders College, Philadelphia, 1992.
27. H. Juntgen, *Carbon,* **15,** 273 (1977).

Received April 22, 1996
Accepted July 16, 1996